International Journal of Heat and Mass Transfer 52 (2009) 3272–3278

Contents lists available at ScienceDirect

International Journal of Heat and Mass Transfer

journal homepage: www.elsevier.com/locate/ijhmt

Analysis of seepage characters in fractal porous media

Meijuan Yun [a,b], Boming Yu [b,*], Jianchao Cai [b]

[a] Department of Applied Physics, Wuhan University of Science and Technology, Wuhan 430081, Hubei, PR China
[b] School of Physics, Huazhong University of Science and Technology, 1037 Luoyu Road, Wuhan 430074, Hubei, PR China

ARTICLE INFO

Article history:
Received 27 May 2008
Received in revised form 13 October 2008
Available online 11 March 2009

Keywords:
Porous media
Fractal
Permeability
Pressure distribution equations

ABSTRACT

In this paper, the plane-radial and plane-parallel flows for Newtonian fluid in fractal porous media are analyzed. Based on the assumption that the porous medium consists of a bundle/set of tortuous streamlines/capillaries and on the fractal characteristics of pore size distribution in porous media, the expressions for porosity, flow rate, velocity and permeability for both radial and parallel flows are developed. The obtained expressions are the functions of tortuosity, fractal dimension, maximum and minimum pore diameters, and there are no empirical constant and every parameter has clear physical meaning in the expressions. The pressure distribution equations for plane-radial and plane-parallel flows in fractal porous media are also derived. The pressure and velocity distributions in plane-radial reservoirs are calculated and discussed.

1. Introduction

Fractal porous media have been studied extensively for more than two decades since Mandelbrot's pioneer work [1]. Katz and Thompson [2] used scanning electron microscopy and optical data to show that the pore spaces of several sandstones are fractal geometries. Fractured rocks [3] and fragmented porous media [4] etc. have also been proved to be fractal objects. It has been shown that fractal geometry theory has been proven to be powerful in analysis of transport properties in porous media with complex and random microstructures [5–8].

The radial flow may exist in many aspects such as oil/water flow toward a well bore, and fluid flow in fractal reservoir [9–11] is thus of central interest to hydrogeologists and petroleum engineers. Tong and Zhang [9] analyzed the pressure behavior of fractal reservoir with dual porosity and gave the exact solutions of pressure distribution for the cases of an infinite outer boundary. Kong et al. [10] studied the fluid flow in porous media with two fractal dimensions and presented the pressure diffusion equation in fractal reservoir. Beier [11] presented a pressure-transient model for a well with a vertical fracture in a fractal reservoir.

The hydraulic conductivity or permeability (hereafter only permeability is mentioned) of porous media has been one of hot topics in the area of porous media. The permeability may be obtained by experiments [12–14] and numerical simulations [15–17]. However, the results from either experiments or numerical simulations are usually correlated as correlations with one or more empirical constants, and the mechanisms behind the constants are thus often ignored. Therefore, the analytical solution for flow and relevant parameters in porous media is desirable.

In this work, based on the tortuous capillaries and the fractal characteristics of pores in porous media, the expressions for porosity, flow rate, velocity and permeability are derived for the plane-radial and plane-parallel flows in fractal porous media. By using the continuity equations and the state equations for slightly compressible fluid, the pressure distribution equations for plane-radial and plane-parallel flows in fractal porous media are also derived.

2. Fractal models for plane-radial flow in isotropic porous media

Fig. 1 shows a coordinate system for radial flow toward the well bore from the outer region. The well bore radius is r_w, h is the reservoir thickness, p and $p + dp$ represent the pressures at distances r and $r + dr$, respectively. The pressure increases with the increase of the radial distance r, so $dp/dr > 0$.

2.1. Pore number

It has been shown that the cumulative size distributions of pores/capillaries in fractal porous media whose pore sizes are greater than or equal to the size λ follow the fractal scaling law [18–20]:

$$N(L \geqslant \lambda) = \left(\frac{\lambda_{\max}}{\lambda}\right)^{D_f} \tag{1}$$

In Eq. (1), $\lambda_{\min} \leqslant \lambda \leqslant \lambda_{\max}$, $\lambda_{\min}$ and $\lambda_{\max}$ are the minimum and maximum pore diameters, D_f is the fractal dimension for pore spaces,

* Corresponding author. Tel./fax: +86 27 87542153.
E-mail address: yuboming2003@yahoo.com.cn (B. Yu).

0017-9310/$ - see front matter © 2009 Elsevier Ltd. All rights reserved.
doi:10.1016/j.ijheatmasstransfer.2009.01.024

Nomenclature

A_0	unit cell area
c	total compressibility
c_f	compressibility of fluid
c_ϕ	compressibility of pore
d	spherical particle diameter
D_f	fractal dimension
h	reservoir thickness
K	permeability
K^+	dimensionless permeability
N	pore number
P	pressure
p^+	dimensionless pressure
p_R	pressure at outer boundary radius
p_w	pressure at well bore
q	flow rate through a single tortuous capillary
Q	total flow rate
r	radial distance
r_w	well bore radius
R	outer boundary radius
V	seepage velocity
V^+	dimensionless velocity

Greek symbols

λ	pore diameter
λ_{max}	maximum pore diameter
λ_{min}	minimum pore diameter
μ	fluid viscosity
ρ	fluid density
τ	tortuosity
ϕ	porosity
ϕ_A	area porosity
ϕ_V	volume porosity
χ	pressure conductivity coefficient

$0 < D_f < 2$ in the two-dimensional space and $0 < D_f < 3$ in the three-dimensional space.

We assume that the cumulative number in a fractal set of capillaries (from a pore diameter λ to the maximum pore diameter λ_{max}) cross a unit cell of area A_0 perpendicular to the flow direction is N, then the total cumulative number of pores on a cylindrical surface of area $A_r = 2\pi rh$ with radius r is

$$N_r = \frac{A_r}{A_0}N = \frac{2\pi rh}{A_0}\left(\frac{\lambda_{max}}{\lambda}\right)^{D_f} \tag{2}$$

Eq. (2) indicates that the larger the radius r, the larger the total number of pores. This is consistent with the practical situation. Differentiating Eq. (2) with respect to λ yields the number of pores whose sizes are within the infinitesimal range λ to $\lambda + d\lambda$ on the cylindrical surface of area A_r

$$-dN_r = \frac{2\pi rh}{A_0}D_f\lambda_{max}^{D_f}\lambda^{-(D_f+1)}d\lambda \tag{3}$$

In Eq. (3), $-dN_r > 0$, which implies that the number of pores decreases with the increase of pore size, and this is consistent with the fractal geometry.

2.2. Porosity

The area porosity at the radial distance r is defined by

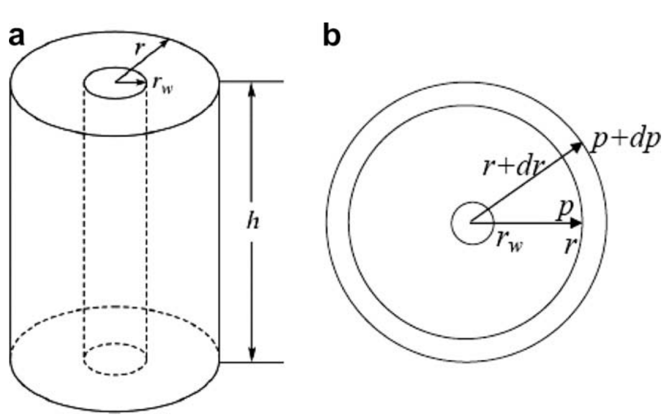

Fig. 1. Coordinate system for the plane-radial flow in isotropic porous media, (a) schematic of a unit cell, and (b) differential element.

$$\phi_A = \frac{A_p}{A_r} = \frac{-1}{2\pi rh}\int_{\lambda_{min}}^{\lambda_{max}}\frac{\pi\lambda^2}{4}dN_r \tag{4}$$

where A_p is the pore area on the cylindrical surface of area A_r, the total pore area is calculated by $A_p = -\int_{\lambda_{min}}^{\lambda_{max}}\frac{\pi\lambda^2}{4}dN_r$.

The volume porosity at the radial distance between r and $r + dr$ is defined by

$$\phi_V = \frac{V_p}{V_t} = \frac{-1}{2\pi rhdr}\int_{\lambda_{min}}^{\lambda_{max}}\frac{\pi\lambda^2}{4}dr_a dN_r \tag{5}$$

where V_p and V_t are, respectively, the pore and total volumes at the radial distance between r and $r + dr$, dr_a is the actual infinitesimal length for radial flow, and dr is the macroscopic or infinitesimal straight length for radial flow. In Eq. (5), $V_p = -\int_{\lambda_{min}}^{\lambda_{max}}\frac{\pi\lambda^2}{4}dr_a dN_r$ and $V_t = 2\pi rhdr$.

Since the streamlines or capillaries in porous media are tortuous, $dr_a \geqslant dr$. The tortuous degree for the streamlines or capillaries is described by tortuosity, which is often defined by [21,22]

$$\tau = L_a/L \tag{6}$$

where L_a and L are the actual length of tortuous flow path and the straight length or thickness of a sample along the macroscopic pressure gradient, respectively. According to Eq. (6), the relation between dr_a and dr can be expressed as

$$dr_a = \tau dr \tag{7}$$

In Eq. (7), an average value τ is taken for a given porous medium, and the tortuosity usually depends on porosity. For the recent models for tortuosity, readers may consult the papers by Yu et al. [23–25].

Inserting Eq. (3) into Eq. (4) results in

$$\phi_A = \frac{\pi D_f}{4(2-D_f)}\frac{\lambda_{max}^2}{A_0}\left[1-\left(\frac{\lambda_{min}}{\lambda_{max}}\right)^{2-D_f}\right] \tag{8}$$

Inserting Eqs. (3) and (7) into Eq. (5) yields

$$\phi_V = \frac{\tau\cdot\pi D_f}{4(2-D_f)}\frac{\lambda_{max}^2}{A_0}\left[1-\left(\frac{\lambda_{min}}{\lambda_{max}}\right)^{2-D_f}\right] \tag{9}$$

Eqs. (8) and (9) present the expressions for area porosity ϕ_A and volume porosity ϕ_V for fractal porous media. Although the derivations of Eqs. (8) and (9) are based on the radial flow, the resultant equations are independent of the radial distance r. This is consistent with the practical situation.

Comparing Eqs. (8) with (9), we have

$$\phi_V = \tau\phi_A \tag{10}$$

Eq. (10) depicts the relationship between the volume porosity and area porosity. Eq. (10) also indicates that when all capillaries are straight ($\tau = 1$), the volume porosity and area porosity are equal, and this is consistent with the practical situation. Eq. (10) also indicates that the volume porosity is higher than the area porosity. It should be noted that Eq. (10) is based on the parallel capillary model. For other models, Eq. (10) may not be valid.

2.3. Seepage velocity

According to the well-known Hagen–Poiseuille equation, the flow rate through a single tortuous capillary can be written as [26]

$$q(\lambda) = \frac{\pi\lambda^4}{128\mu}\frac{dp}{dr_a} \tag{11}$$

where μ is the fluid viscosity and dp/dr_a is pressure gradient along a tortuous path/capillary.

The total flow rate across the cylindrical surface of area A_r is

$$Q = -\int_{\lambda_{\min}}^{\lambda_{\max}} q(\lambda)dN_r \tag{12}$$

Substituting Eqs. (3), (7), and (11) into Eq. (12), we have

$$Q = \frac{\pi^2 D_f \lambda_{\max}^4}{64\mu\tau(4-D_f)}\frac{rh}{A_0}\frac{dp}{dr}\left[1-\left(\frac{\lambda_{\min}}{\lambda_{\max}}\right)^{4-D_f}\right] \tag{13}$$

Since $0 < D_f < 2$ in the two-dimensional space, the exponent $4 - D_f > 2$, in general $\lambda_{\min}/\lambda_{\max} < 10^{-2}$, so $(\frac{\lambda_{\min}}{\lambda_{\max}})^{4-D_f} << 1$. Then Eq. (13) is reduced to

$$Q = \frac{\pi^2 D_f \lambda_{\max}^4}{64\mu\tau(4-D_f)}\frac{rh}{A_0}\frac{dp}{dr} \tag{14}$$

Then, the seepage (average) velocity V for radial flow in fractal porous media can be obtained by

$$V = \frac{Q}{A_r} = \frac{Q}{2\pi rh} = \frac{\pi D_f \lambda_{\max}^2}{128\mu\tau(4-D_f)}\frac{\lambda_{\max}^2}{A_0}\frac{dp}{dr} \tag{15}$$

Eq. (15) indicates that the radial velocity depends on the pressure gradient, microstructural parameters and fluid property.

2.4. Permeability

The Darcy's law for the radial flow is expressed as

$$V = -\frac{K}{\mu}\frac{dp}{dr} \tag{16}$$

where K is the permeability, and the minus sign represents the direction of the seepage velocity is opposite to the pressure gradient.

By comparing Eq. (15) with Eq. (16), we obtain the permeability expression for the radial flow in fractal porous media as

$$K = \frac{\pi D_f}{128\tau(4-D_f)}\frac{\lambda_{\max}^4}{A_0} \tag{17}$$

Eq. (17) shows that the permeability is independent of the radial distance r, and it depends on the pore fractal dimension, tortuosity and the microstructural parameters of porous media.

From Eq. (17), the dimensionless permeability may be expressed as

$$K^+ = \frac{K}{d^2} = \frac{\pi D_f \lambda_{\max}^4}{128\tau(4-D_f)A_0 d^2} \tag{18}$$

where d is the average diameter of particles. It is seen that the permeability Eq. (18) strongly depends on the maximum pore size. The available models for maximum pore size will be given in Section 4.

2.5. The pressure distribution equation

If the slightly compressible fluid flow in fractal porous media is assumed, the equation of state is [21]

$$\rho = \rho_0 e^{c_f\Delta p} \cong \rho_0(1 + c_f\Delta p) \tag{19}$$

where the pressure difference is $\Delta p = p(r,t) - p_0$, $p(r,t)$ is the pressure at the radial distance r and time t, ρ is the density of fluid, ρ_0 is the fluid density at the reference pressure p_0, and c_f (in the order of $10^{-4}/10^{-5}$ MPa^{-1} [27]) is the compressibility of fluid.

For general porous media, if the compressibility of pores is involved, the porosity may be expressed as [21,28]

$$\phi = \phi_0(1 + c_\phi\Delta p) \tag{20}$$

where φ_0 is the porosity at the reference pressure p_0, and c_φ denotes compressibility of pore.

Multiplying Eq. (19) by Eq. (20) yields

$$\rho\phi = \rho_0\phi_0(1 + c\Delta p + c_f c_\phi \Delta p^2) \tag{21}$$

In Eq. (21), $c = c_f + c_\phi$ is the total compressibility.

Since the compressibility (c_f or c_ϕ) is generally in the order of $10^{-4}/10^{-5}$, the product $c_f c_\phi$ is about in the order of $10^{-8}/10^{-10}$, which is far less than 1. Thus, the second-order term $c_f c_\phi \Delta p^2$ in Eq. (21) can be omitted, and then Eq. (21) can be reduced to

$$\rho\phi = \rho_0\phi_0(1 + c\Delta p) \tag{22}$$

The continuity equation for the radial flow is given by

$$\frac{\partial(\rho\phi)}{\partial t} + \frac{1}{r}\frac{\partial}{\partial r}(r\rho V) = 0 \tag{23}$$

Based on Eqs. (16), (19), and (22), Eq. (23) can be rewritten as the classic form of pressure distribution equation for radial flow, i.e.

$$\frac{\partial^2 p}{\partial r^2} + \frac{1}{r}\frac{\partial p}{\partial r} = \frac{1}{\chi}\frac{\partial p}{\partial t} \tag{24a}$$

where χ is called the pressure conductivity coefficient:

$$\chi = \frac{K}{\phi_0\mu c} \tag{24b}$$

It can be seen from Eq. (24) that the pressure conductivity coefficient is related to the permeability, porosity, compressibility and viscosity. In the present model the permeability K is determined by Eq. (17), which has no empirical constant, and more physical mechanisms are revealed. Eq. (24) with proper boundary conditions can be solved for the pressure distribution.

If an incompressible fluid flow in porous media is involved, the fluid density is a constant, $c_f = 0$, then Eq. (24b) can be written as

$$\chi = \frac{K}{\phi_0\mu c_\phi} \tag{24c}$$

Eq. (24c) is the pressure conductivity coefficient for incompressible fluid.

Although Eq. (24) is formally the same as that appearing in textbooks on porous medium, the permeability K in Eq. (24) is involved with the fractal natures. And, although the pressure distribution equation discussed in this section is based on slightly compressible fluid for general consideration, it is easy to extend to that for incompressible fluid. In result sections, we only consider the incompressible fluid and steady state flow for simplicity.

2.6. Dimensionless pressure and velocity

Assume that the pressure p is independent of time t and the flow is toward a well from radial distance R. Then, the pressure distribution equation and boundary conditions for plane-radial flow can be obtained from Eq. (24) as

$$\frac{d^2p}{dr^2}+\frac{1}{r}\frac{dp}{dr}=0 \quad (r_w \leqslant r \leqslant R) \tag{25}$$

$$p(r=r_w)=p_w \tag{26}$$

$$p(r=R)=p_R \tag{27}$$

where R is the radius of a cylindrical region into which fluid flows, p_w is the pressure at well bore, p_R is the pressure at radial distance R, and $p_R > p_w$.

According to Eqs: (25)–(27), the radial pressure distribution is obtained as

$$p(r)=p_w+(p_R-p_w)\frac{\ln(r/r_w)}{\ln(R/r_w)} \tag{28a}$$

The pressure gradient is

$$\frac{dp}{dr}=\frac{1}{r}\frac{p_R-p_w}{\ln(R/r_w)}(>0) \tag{28b}$$

Eq. (28) indicates that the pressure increases with the distance r, but the value of the pressure gradient (dp/dr) decreases with the increase of the radial distance r, and the pressure gradient approaches zero as r tends to infinity because the pressure p_R at infinity remains finite.

Inserting Eq. (28b) into Eq. (15) results in

$$V=\frac{\pi D_f(p_R-p_w)\lambda_{\max}^4}{128\mu\tau r(4-D_f)\ln(R/r_w)A_0} \tag{29}$$

Eq. (29) reveals that the average (superficial) velocity decreases with the radial distance r, and due to the same reason as for the pressure gradient, the radial velocity at the infinity approaches zero. Eq. (29) also shows that when the fractal dimension is D_f = 2, the velocity reaches the maximum value. This is interpreted as that when the fractal dimension reaches D_f = 2, a unit cell is completely occupied by pores and no solid phase/particle exists in the space (in this situation the area porosity is unity), leading to the maximum velocity for flow. In addition, when porosity is unity, the streamlines become straight, and thus the tortuosity reaches the minimum value of 1. This also causes the minimum flow resistance and thus maximum velocity. Eq. (29) indicates that the radial velocity is related to the structural parameters (D_f, r, τ, $\lambda_{\max}$, R and r_w) of a porous medium, fluid property (μ), and pressure difference between two points. It is seen that the possible factors affecting the velocity in porous media are fully revealed, and every parameter in Eq. (29) has clear physical meaning. However, since the conventional method defines the velocity in porous media by the volume average [21], and the effects of the microstructural parameters on flow velocity in porous media are often ignored.

From Eqs. (28a) and (29), the dimensionless pressure and velocity distribution equations for radial flow, respectively, are

$$p^+=\frac{p(r)}{p_w}=1+\left(\frac{p_R}{p_w}-1\right)\frac{\ln(r^+)}{\ln(R/r_w)} \tag{30}$$

$$V^+=\frac{V}{\frac{d^2}{\mu}\frac{p_w}{r_w}}=\frac{\pi D_f\left(\frac{p_R}{p_w}-1\right)\lambda_{\max}^4}{128\tau(4-D_f)\ln(R/r_w)A_0d^2}\frac{1}{r^+} \tag{31}$$

where $r^+ = r/r_w$ is dimensionless radial distance.

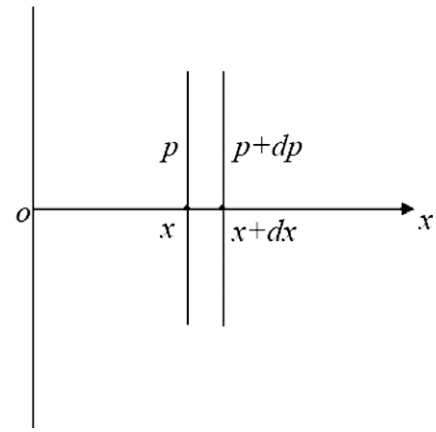

Fig. 2. Coordinate system for the plane-parallel flow in isotropic porous media.

3. Fractal models for plane-parallel flow in isotropic porous media

Fig. 2 shows a coordinate system for parallel flow along the x-axis direction. p and $p + dp$ represent the pressures at the coordinates x and $x + dx$, respectively. The pressure decreases with the increase of the horizontal distance, so $dp/dx < 0$.

3.1. Pore number

The number of pores whose diameters are within the infinitesimal range λ to $\lambda + d\lambda$ in the cross-sectional area A

$$-dN_A=\frac{A}{A_0}D_f\lambda_{\max}^{D_f}\lambda^{-(D_f+1)}d\lambda \tag{32}$$

Eq. (32) shows that the pore number is independent of the horizontal distance x and is only related to the cross-sectional area and microstructural parameters.

3.2. Porosity

For plane-parallel flow, the area porosity ϕ_A and volume porosity ϕ_V are exactly the same as Eqs. (8,9,10). This can be explained that the structural parameters ($\lambda_{\min}$, $\lambda_{\max}$, D_f, τ and A_0) for pores/capillaries are the same in different coordinate systems, and porosity is a macroscopic parameter which is independent of the coordinate system chosen.

3.3. Seepage velocity

By the similar way with radial flow, the seepage (average) velocity V for parallel flow in porous media is obtained as

$$V=\frac{Q}{A}=\frac{\pi D_f\lambda_{\max}^2}{128\mu\tau(4-D_f)}\frac{\lambda_{\max}^2}{A_0}\left(-\frac{dp}{dx}\right) \tag{33a}$$

where $-dp/dx > 0$. Eq. (33a) denotes that the seepage (average) velocity is related to the microstructures of porous media and pressure gradient. Eq. (33a) also shows that the velocity keeps unchanged when the pressure gradient is a constant. For anisotropic porous media, the velocities in x-, y- and z-directions may be different, and then we have the velocity equation in the vector form

$$\vec{V}=-\frac{\pi D_f\lambda_{\max}^2}{128\mu\tau(4-D_f)}\frac{\lambda_{\max}^2}{A_0}\nabla p \tag{33b}$$

where $\vec{V}=V_x\vec{i}+V_y\vec{j}+V_z\vec{k}$, and V_x, V_y and V_z are the velocity components in the x-, y-, and z-directions, respectively. In this situation, the parameters in different directions are inserted into Eq. (33b), then the seepage (average) velocities in x-, y- and z-directions can be obtained, respectively. Compared Eq. (33a) with Eq. (15), the seepage velocity depends not only on the geometrical parameters of porous media but also on the pressure gradient ($\partial p/\partial r$ or $-\partial p/\partial x$), and the coefficient before the pressure gradient in Eqs. (15) and (33a) is the same. This is expected.

3.4. Permeability

The Darcy's law for the plane-parallel flow is expressed as

$$V_x = \frac{K}{\mu}\left(-\frac{dp}{dx}\right) \tag{34}$$

By comparing Eq. (33a) with Eq. (34), we obtain the permeability expression for the plane-parallel flow which is exactly the same as Eq. (17). This shows that the permeability is independent of the spatial coordinate and fluid properties, and it only depends on the inherent structural parameters of porous media.

3.5. The pressure distribution equation

The continuity equation for the parallel flow is given by

$$\frac{\partial(\rho\phi)}{\partial t} + \frac{\partial}{\partial x}(\rho V_x) = 0 \tag{35}$$

Based on Eqs. (19), (22), and (34), Eq. (35) can be rewritten as the classic form of pressure distribution equation for parallel flow

$$\frac{\partial^2 p}{\partial x^2} = \frac{1}{\chi}\frac{\partial p}{\partial t} \tag{36a}$$

where χ is exactly the same as Eq. (24b). This is expected because the permeability, porosity, viscosity and compressibility are all independent of the coordinate system chosen.

Eq. (36) can be further written as the general form in three dimensions as follows:

$$\nabla^2 p = \frac{1}{\chi}\frac{\partial p}{\partial t} \tag{36b}$$

where $\nabla^2 p = \partial^2 p/\partial x^2 + \partial^2 p/\partial y^2 + \partial^2 p/\partial z^2$, Eq. (36) with proper boundary conditions can be solved for the pressure distribution.

3.6. Dimensionless pressure and velocity

For steady state flow, by solving the pressure distribution equation with boundary conditions ($p(x = 0) = p_0$ and $p(x = L) = p_L$), we obtain the pressure distribution expression for plane-parallel flow

$$p(x) = p_0 - (p_0 - p_L)\frac{x}{L} \tag{37a}$$

where L is the length of a medium/sample.

The pressure gradient is

$$\frac{dp}{dx} = \frac{p_L - p_0}{L}(< 0) \tag{37b}$$

From Eq. (37) we can see that the pressure decreases linearly with the distance, but the value of the pressure gradient is independent of the horizontal distance x.

Inserting Eq. (37) into Eq. (33a) yields

$$V = \frac{\pi D_f (p_0 - p_L)\lambda_{max}^4}{128\mu L\tau(4 - D_f)A_0} \tag{38}$$

where $p_0 > p_L$. Eq. (38) shows that the velocity is proportional to the pressure drop between two points in a medium. Eq. (38) also indicates that the horizontal velocity is related to the structural parameters of porous media, but it is independent of the horizontal coordinate x. There is no empirical constant and every parameter in Eq. (38) has clear physical meaning.

From Eqs. (37a) and (38), the dimensionless pressure and velocity distribution equations for parallel flow are expressed, respectively, as

$$P^+ = \frac{p(x)}{p_0} = 1 - \left(1 - \frac{p_L}{p_0}\right)\frac{x}{L} \tag{39}$$

$$V^+ = \frac{V}{\frac{d^2}{\mu}\frac{p_L}{L}} = \frac{\pi D_f\left(\frac{p_0}{p_L} - 1\right)\lambda_{max}^4}{128\tau(4 - D_f)A_0 d^2} \tag{40}$$

4. Results and discussion

Now, the fractal models for velocity, permeability and pressure distribution equations have been obtained analytically. It is seen that the models presented in this work do not contain any empirical constant and every parameter has clear physical meaning. However, the determination of these quantities such as velocity, permeability and pressure distributions in a porous medium depends on the availability of other parameters such as τ, λ_{max}, D_f and A_0.

A correlation between the average tortuosity of flow path and porosity was given by [29]

$$\tau = 1 + 0.41\ln(1/\phi_V) \tag{41}$$

which was obtained by the experiments on flow through beds packed with spherical particles. According to Eq. (41), the tortuosity can be calculated if porosity is determined.

The minimum pore diameter λ_{min} can be obtained when three circular particles touching each other

$$\lambda_{min} = d\sqrt{\frac{\sqrt{3}}{\pi} - \frac{1}{2}} \tag{42}$$

The maximum pore diameter λ_{max} may be obtained when circular particles are arranged in an equilateral-triangle array as [18]

$$\lambda_{max1} = \frac{d}{4}\left[\sqrt{\frac{2\phi_A}{1 - \phi_A}} + \sqrt{\frac{2\pi}{\sqrt{3}(1 - \phi_A)}} - 2\right] \tag{43a}$$

The maximum pore diameter λ_{max} may also be obtained when circular particles are arranged in a square array as [30]

$$\lambda_{max2} = d\sqrt{\frac{\phi_A}{1 - \phi_A}} \tag{43b}$$

If the maximum pore size is chosen to be the average value over Eqs. (43a) and (43b), the average maximum pore diameter can be obtained as

$$\lambda_{max} = (\lambda_{max1} + \lambda_{max2})/2 \tag{43c}$$

So far, no generally accepted maximum pore size model is presently available in literature.

The pore area fractal dimension D_f can be determined by [19]

$$D_f = 2 - \frac{\ln\phi_A}{\ln(\lambda_{min}/\lambda_{max})} \tag{44}$$

Once λ_{min} and λ_{max} are obtained by Eqs. (42) and (43c) and porosity is given, the fractal dimension D_f can be calculated from Eq. (44).

The total pore area in a unit cell A_0 can be obtained with the aid of Eqs. (1) and (44)

$$A_{p0} = \int_{\lambda_{min}}^{\lambda_{max}} \frac{\pi\lambda^2}{4}(-dN) = \frac{\pi D_f\lambda_{max}^2}{4(2 - D_f)}(1 - \phi_A) \tag{45}$$

where $-dN$ can be determined by differentiating Eq. (1), and $-dN = D_f \lambda_{\max}^{D_f} \lambda^{-(D_f+1)} d\lambda$. The unit cell area A_0 is then calculated by

$$A_0 = \frac{A_{p0}}{\phi_A} = \frac{1-\phi_A}{\phi_A} \frac{\pi D_f \lambda_{\max}^2}{4(2-D_f)} \tag{46}$$

In calculation of pressure, velocity and permeability, once porosity is given, the parameters τ, $\lambda_{\max}$, D_f and A_0 are determined by Eqs. (41), (43c), (44), and (46), respectively. Then, the dimensionless permeability, pressure distribution and velocity for radial flow can be found from Eqs. (18), (30), and (31), respectively. The well bore and outer boundary radii are respectively assumed to be r_w = 0.1 m and R = 100 m. The results will be compared with those predicted by Ergun's equation.

From the well-known Ergun's equation, the dimensionless permeability can be obtained as [31]

$$K^+ = \frac{\phi_V^3}{150(1-\phi_V)^2} \tag{47}$$

The Ergun's equation has hotly been debated in the area of porous media in the past decades. The empirical constant in Ergun's equation was thought to be 150–250 obtained by different researchers [31–34], and interested readers may consult Refs. [31–35] for detail.

Fig. 3 compares the predictions by the present fractal model Eq. (18) with Ergun's relation Eq. (47). Fig. 3 shows that the permeability obtained by Eq. (18) may be lower or higher than that by Eq. (47) when the different models (Eq. (43a), (43b)) for the maximum pore diameters are applied. When the model Eq. (43c) for the averaged maximum pore diameter is used, the predicted permeability by Eq. (18) is closer to that by Eq. (47). In all, the present model Eq. (18) may qualitatively present an agreement with Ergun's equation.

Fig. 4 denotes the relationship between the dimensionless pressure p^+ and the dimensionless radial distance r^+ by Eq. (30) for radial flow. The dimensionless pressure p^+ increases with the increase of r^+ and the ratio of p_R/p_w. This is consistent with the physics situation.

For calculation of flow velocity by Eq. (29), we here give an example. In a general reservoir, $p_R - p_w$ = 1 MPa when R = 100 m and r_w = 0.1 m [36], and if we assume $\phi_V = 0.3$, d = 1 mm and μ = 2 $\times 10^{-3}$ Pa s, the other parameters τ, $\lambda_{\min}$, $\lambda_{\max}$, D_f and A_0 in Eq. (29) can be obtained accordingly, then the values of velocity V can be obtained to be 0.31 m/s, 0.031 m/s, 0.0031 m/s and 0.00031 m/s at different radial distances r = 0.1 m, 1 m, 10 m and 100 m, respectively. When $p_R - p_w$ = 10 MPa, the values of velocity V are 3.1 m/s, 0.31 m/s, 0.031 m/s and 0.0031 m/s at different radial distances r = 0.1 m, 1 m, 10 m and 100 m, respectively.

The dimensionless radial flow velocity by Eq. (31) is shown in Figs. 5 and 6. It can clearly be seen from Figs. 5 and 6 that the dimensionless seepage velocity V^+ drops sharply with the increase

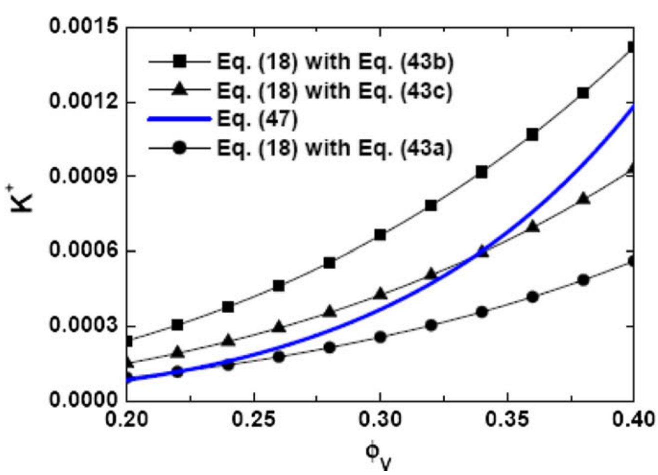

Fig. 3. A comparison between the present model predictions and those predicted by Ergun's equation.

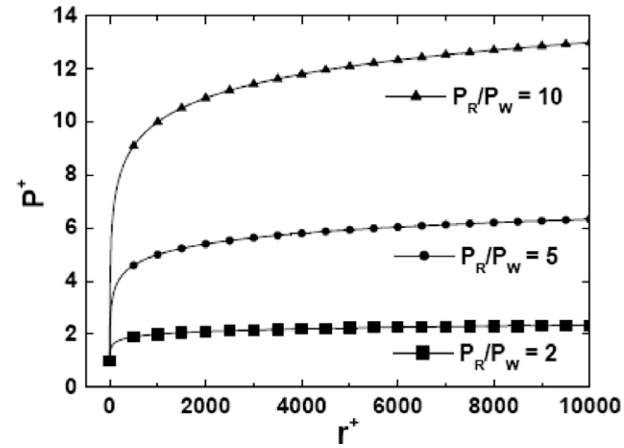

Fig. 4. The dimensinoless pressure P^+ versus the dimensionless radial distance r^+ at different ratios of p_R/p_w for radial flow.

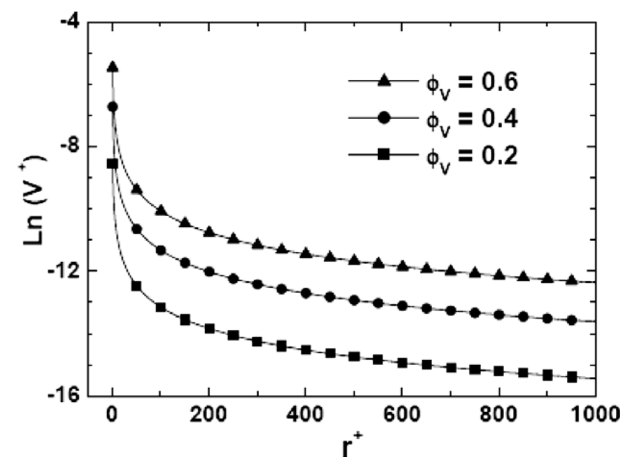

Fig. 5. The dimensinoless velocity V^+ versus the dimensionless radial distance r^+ at different volumes porosities as p_R/p_w = 10 for radial flow.

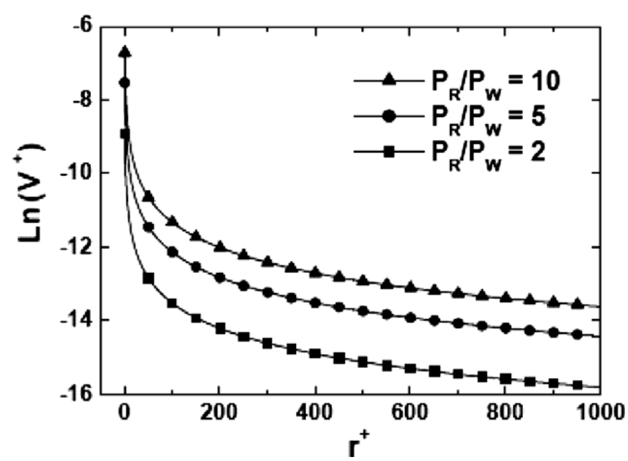

Fig. 6. The dimensinoless velocity V^+ versus the dimensionless radial distance r^+ at different ratios of p_R/p_w as Φ_v = 0.4 for radial flow.

of the dimensionless radial distance r^+ and approaches zero when r^+ tends to infinity. Fig. 5 also shows that the velocity increases with the increase of porosity. Fig. 6 denotes that the velocity increases with the ratio of p_R/p_w. These results are consistent with the physical situations.

5. Conclusions

In this paper, we have derived the plane-radial and plane-parallel flows for Newtonian fluid flow in fractal porous media. Based on the assumption that the porous medium consists of a bundle/set of tortuous streamlines/capillaries and on the fractal characteristics of pore size distribution in porous media, the fractal expressions for porosity, flow rate, velocity and the permeability for both radial flow and parallel flow have been obtained. We have also derived the pressure distribution equations for the slightly compressible fluid in fractal porous media. The dimensionless analytical expressions for permeability, pressure and velocity are obtained. The obtained expressions are the functions of tortuosity, pore area fractal dimension, fluid property, maximum and minimum pore diameters, and every parameter has clear physical meaning.

Acknowledgement

This work was supported by the National Natural Science Foundation of China through Grant No. 10572052.

References

[1] B.B. Mandelbrot, The Fractal Geometry of Nature, Freeman, New York, 1982.
[2] A.J. Katz, A.H. Thompson, Fractal sandstone pores: implication for conductivity and pore formation, Phys. Rev. Lett. 54 (1985) 1325–1328.
[3] M. Sahimi, Flow phenomena in rocks: from continuum models to fractals percolation, cellular, automata, and simulated annealing, Rev. Modern Phys. 65 (1993) 1393–1534.
[4] C.O. Karacan, P.M. Halleck, A fractal model for predicting permeability around perforation tunnels using size distribution of fragmented grains, J. Petrol Sci. Eng. 40 (2003) 159–176.
[5] B.M. Yu, Fractal dimensions for multiphase fractal media, Fractals 14 (2006) 111–118.
[6] B. Zhang, B.M. Yu, H.X. Wang, M.J. Yun, A fractal analysis of permeability for power-law fluids in porous media, Fractals 14 (2006) 171–177.
[7] X.Y. Li, B.E. Logan, Permeability of fractal aggregates, Water Res. 35 (2001) 3373–3380.
[8] Y.J. Liu, B.M. Yu, A fractal model for relative permeability of unsaturated porous media with capillary pressure effect, Fractals 15 (2007) 217–222.
[9] D.K. Tong, H.Q. Zhang, The flow problem of fluids flow in a fractal reservoir with double porosity, Appl. Math. Mech. 22 (2001) 1118–1126.
[10] X.Y. Kong, D.L. Li, D.T. Lu, Basis formulas of fractal seepage and type-curves of fractal reservoirs, J. Xian Shiyou Univ. 22 (2007) 1–5. in Chinese.
[11] R.A. Beier, Pressure-transient model for a vertically fractured well in a fractal reservoir, SPEFE 9 (1994) 122–128.
[12] J. Levec, A.E. Saez, R.G. Carbonell, The hydrodynamics of tricking flow in packed beds. Part II: experimental observations, AIChE J. 32 (1986) 369–380.
[13] T.J. Wang, C.H. Wu, L.J. Lee, In-plane permeability measurement and analysis in liquid composite molding, Polym. Compos. 15 (1994) 278–288.
[14] Z.Q. Chen, P. Cheng, T.S. Zhao, An experimental study of two phase flow and boiling heat transfer in bi-dispersed porous channels, Int. Commun. Heat Mass Transfer 27 (2000) 293–302.
[15] R. Benzi, S. Succi, M. Vergassola, The lattice Boltzmann equation: theory applications, Phys. Rep. 222 (1992) 145–197.
[16] P.M. Adler, B. Berkowitz, Effective medium analysis of random lattices, Trans. Porous Media 40 (2000) 145–151.
[17] R.B. Pandey, J.L. Becklehimer, J.F. Gettrust, Density profile and flow of driven gas in an open porous medium with a computer simulation, Phys. A. 289 (2001) 321–335.
[18] B.M. Yu, P. Cheng, A fractal permeability model for bi-dispersed porous media, Int. J. Heat Mass Transfer 45 (2002) 2983–2993.
[19] B.M. Yu, J.H. Li, Some fractal characters of porous media, Fractals 9 (2001) 365–372.
[20] B.M. Yu, L.J. Lee, H.Q. Cao, A fractal in-plane permeability model for fabrics, Polym. Compos. 22 (2002) 201–221.
[21] J. Bear, Dynamics of Fluids in Porous Media, Elsevier, New York, 1972.
[22] F.A.L. Dullien, Porous Media: Fluid Transport and Pore Structure, Academic Press, London, 1979.
[23] B.M. Yu, J.H. Li, A geometry model for tortuosity of flow path in porous media, Chinese Phys. Lett. 21 (2004) 1569–1571.
[24] M.J. Yun, B.M. Yu, B. Zhang, M.T. Huang, A geometry model for tortuosity of streamtubes in porous media with spherical particles, Chinese Phys. Lett. 22 (2005) 1464–1467.
[25] M.J. Yun, B.M. Yu, P. Xu, J.S. Wu, Geometrical models for tortuosity of streamlines in three dimensional porous media, Can. J. Chem. Eng. 84 (2006) 301–309.
[26] M.M. Denn, Process Fluid Mechanics, Prentice-Hall, New Jersey, 1980.
[27] X.Y. Kong, Advanced Mechanics of Fluids in Porous Media, Press of University of Science and Technology of China, Hefei, China, 1999.
[28] H.N. Hall, Compressibility of reservoir rocks, Trans. AIME 198 (1953) 309–316.
[29] J. Comiti, M. Renaud, A new model for determining mean structure parameters of fixed beds from pressure drop measurements: application to beds packed with parallelepipedal particles, Chem. Eng. Sci. 44 (1989) 539–1545.
[30] J.S. Wu, B.M. Yu, A fractal resistance model for flow through porous media, Int. J. Heat Mass Transfer 50 (2007) 3925–3932.
[31] S. Ergun, Fluid flow through packed columns, Chem. Eng. Prog. 48 (1952) 89–94.
[32] I.F. MacDonald, M.S. EL-Sayed, K. Mow, F.A.L. Dullien, Flow through porous media – the Ergun equation revised, Ind. Eng. Chem. Fund 18 (1979) 199–208.
[33] J.P. Du Plessis, Analytical quantification of coefficients in the Ergun equation for fluid friction in a packed bed, Trans. Porous Media 16 (1994) 189–207.
[34] R.E. Hicks, Pressure drop in packed beds of spheres, Ind. Eng. Chem. Fund 9 (1970) 500–502.
[35] J.S. Wu, B.M. Yu, M.J. Yun, A resistance model for flow through porous media, Trans. Porous Media 71 (3) (2008) 331–343.
[36] J.G. Zhang, G.L. Lei, Y.Y. Zhang, Seepage Mechanics of Oil–Gas Reservoirs, Press of Petroleum University, Beijing, China, 2004. p. 39.